Accuracy of Electroencephalographic Dipole Localization of Epileptiform Activities Associated with Focal Brain Lesions

Timo Krings,* Keith H. Chiappa, MD,* B. Neil Cuffin, PhD,†
Bradley R. Buchbinder, MD,‡ and G. Rees Cosgrove, MD§

We evaluated the accuracy of an electroencephalographic (EEG) localization technique (dipole inverse solution) in a consecutive series of 12 focal intracerebral lesions of diverse etiologies whose EEGs showed interictal spike activity or rhythmic activity at seizure onset. The calculated equivalent dipole was plotted on three axes in the patients' magnetic resonance image, and the distance between the dipole and the lesion margin was measured assuming that the shell of the lesion constituted an epileptogenic region. In all cases the dipole localized closer than 0.8 cm to the nearest lesion margin. In addition, we compared the postsurgical outcome of 6 patients to the dipole localization and the resection margins. In all 6 patients in whom the dipole, and hence the estimated seizure generator, was removed the surgical outcome was favorable. We conclude that the inverse solution algorithm is a promising method for using the scalp EEG to localize the sources of electrical activity in the human brain in routine clinical electroencephalography and provides three-dimensional data not available from conventional analysis.

Krings T, Chiappa KH, Cuffin BN, Buchbinder BR, Cosgrove GR. Accuracy of electroencephalographic dipole localization of epileptiform activities associated with focal brain lesions. Ann Neurol 1998;44:76–86

Electrical sources in the human brain produce volume-conducted fields that can be registered using scalp electrodes. From the shape and magnitude of the scalp-recorded voltage fields, the three-dimensional locations of the recording electrode array and the different conductivities of brain, skull, and scalp, an inverse solution can be calculated for the location of the equivalent point source within the brain. This solution is calculated by iteratively adjusting the location, orientation, and amplitude of a source in a model of the head to obtain the best fit between the recorded EEG and those produced by the source in the head model. Once a head and source model have been specified, there is only one source location, orientation, and amplitude that produces the best fit between the actual electroencephalogram (EEG) results and the values produced by the model. The inverse solution algorithm can get "trapped" at a local best fit, but this fit is not as good as the global best fit, unless excessive noise is present.

Electrical source analysis was used by Scherg and Buchner[1–3] to localize electromagnetic evoked potentials to auditory and somatosensory stimuli in normal subjects. Temporally overlapping activities from the brainstem and thalamus and from multiple sources in the region of the contralateral auditory and somatosensory projection areas were revealed by correlating the modeled sources to the brain anatomy.

Ebersole[4] used EEG dipole modeling to assess the character of cerebral generators of EEG spikes and seizure rhythms and correlated these predictions with intracranial EEG recordings. Patients with mesial temporal sclerosis had spikes with oblique and stable equivalent dipoles, patients with discrete cortical lesions had spikes with radial and stable dipoles, whereas patients with extensive or multifocal cortical lesions had spikes with radial and unstable dipoles.[4,5] These authors concentrated on the directional components of the dipoles rather than on their precise localization.

The accuracy with which electrical sources in the human brain can be localized noninvasively using a single moving dipole inverse solution algorithm has been assessed previously.[6–9] They generated artificial dipoles in the brain of patients with implanted depth electrodes and were able to determine that their localization had an average error of 10 to 20 mm.

In the clinical setting, dipole localization accuracy was assessed by correlating the calculated dipoles to

From the *Clinical Neurophysiology Laboratory of the Neurology Service, †Francis Bitter Magnet Laboratory, MIT, ‡Neuroradiology Division in the Department of Radiology, and §Neurosurgical Service, Massachusetts General Hospital, Boston, MA.

Received Jun 7, 1997, and in revised form Oct 26. Accepted for publication Jan 27, 1998.

Address correspondence to Dr Chiappa, EEG Laboratory, Massachusetts General Hospital, Boston, MA 02114.

electrocorticography (ECoG) findings in a few patients and it was found that the dipoles localized to positions that were in accordance with the ECoG localizations.[10,11] In neither paper was there an exact description of the localization accuracy. It has been demonstrated that epileptogenic regions are found near structural lesions.[12,13] However, no study has attempted to correlate the localization of structural lesions to the dipole localization to determine its accuracy.

In this paper we report 12 consecutive cases of patients with focal intracerebral lesions and EEG abnormalities that we used for dipole modeling. We describe the method used for localizing electrical sources in the brain and for plotting them on the patients' magnetic resonance image and validate the inverse solution algorithm by correlating our findings with radiological and pathological data.

Patients and Methods

We selected patients from the routine clinical EEG laboratory who met two criteria: (1) their EEGs demonstrated interictal spikes or rhythmic activity at seizure onset, and (2) they had a focal lesion on magnetic resonance imaging (MRI) or computed tomography (CT). Patients with multiple spike foci or diffuse pathology were excluded. No patient or seizure, once accepted for the study on the basis of suitable spikes or seizure onset in the EEG and a focal lesion on CT or MRI, was later excluded from the data presented in the results. Thus, given those procedures for patient selection, this was a consecutive series of patients. Of the 12 patients investigated, 5 had mesial temporal sclerosis (as demonstrated by high-resolution coronal MRI and surgical pathology), 2 had low-grade tumors in the frontal lobe, and 1 each had postinfarction cavitary and gliotic changes in the parietal lobe, temporal scar tissue secondary to an old temporal lobectomy, frontal heterotopic gray matter, an intracerebral hemorrhage in the superior frontal lobe, and an area of dysplastic gray matter with focal gliosis in the inferior part of the parietal lobe. In 4 patients, rhythmic activity during seizure onset was evaluated, and in the remaining 8, interictal spikes were used for dipole modeling.

EEG Acquisition

Digital EEGs were recorded from 21 electrodes placed according to the International 10-20 system applied with standard techniques. The common reference was either the C2 cervical spine or a balanced neck-chest derivation.[14] Bandpass filter settings were from 0.1 to 100 Hz. If seizure onset activity was evaluated, additional bandpass digital filtering was used at the investigator's discretion, especially if excessive muscle artifact was present. Sample rate was 240/sec with 12-bit resolution. Scalp negativity produced an upward trace deflection and decreasing amplitude values.

Signal Averaging

We chose an EEG channel that showed the earliest, most-consistent and highest-amplitude waveforms and marked the events, always in this channel, by placing a cursor on the negative peak. These events were then superimposed so that the operator could reject erroneously marked events and spikes that had a clearly different appearance (usually due to artifact). The data were then averaged, the resultant waveform was displayed, and the peak was marked with a cursor. The amplitude at that timepoint was then calculated for each channel relative to a baseline determined by averaging all samples in that channel over the entire selected EEG segment, usually 2 to 3 minutes. Typically, 20 spikes or 80 rhythmic waves were averaged (spikes—minimum 12, maximum 144, median 21; rhythmic waves—minimum 38, maximum 133, median 80). The amplitude values for the channels were then used as the input for the inverse solution algorithm. Relative scalp negativity produced an upward deflection on the EEG according to the polarity convention used by electroencephalographers.

The Inverse Solution Algorithm

The electrical sources in the brain were computed using the single moving dipole inverse solution algorithm (ISA).[6,8,15,16] We always performed this step of the evaluation before we viewed the MR image or CT scan of the patient in any detail. The ISA iteratively determined the best fit between the recorded EEG and the calculated potential of a single electrical point source in the brain whose location, direction, and amplitude were varied.[17] The operator freely chose the point in the head from which the program started to calculate the intracranial source. The program then iteratively calculated the solution with the best fit closest to this first estimation. A robust solution (eg, with a high signal-to-noise ratio) resulted in the same solution no matter where in the head the operation was initiated, whereas a weak solution showed a large variability. As a measure of the percentage of the data that was explained by the solution of the dipole location, the goodness of fit was calculated as described in a previous paper.[8] The goodness of fit gave the operator a general idea whether the solution was usable. In our series of patients, the amount of data that remained unexplained ranged from 40% to 9% (median, 21%). However, the utility of this value should not be overestimated because the magnitude of the goodness of fit value cannot be taken as an indication that the localization error is small.[8,18,19]

The solutions were obtained in a four-shell spherical head model, with the shells representing the brain, cerebrospinal fluid (CSF), skull, and scalp. The radii and conductivities of the four concentric regions were brain = 8.2 cm, 0.33 mhos/m; CSF = 8.4 cm, 1.0 mhos/m; skull = 9.0 cm, 0.0042 mhos/m; and scalp = 10 cm, 0.33 mhos/m.[20,21]

Determination of the Coordinate System of the Subject's Head and Plotting of the Dipole on MRI/CT

The results of the inverse solution algorithm were located on a coordinate system that was defined by the position of the recording electrodes. These electrodes were applied to the scalp according to the International 10-20 system, which was based on anatomical landmarks of the individual's head. The x axis (anterior to posterior) was defined by a line through FPZ and OZ, the y axis (left to right) was defined by the line through T3 and T4, and the z axis was defined by the line

through the intersection of the x and y axes and the CZ electrode position. The electrode positions and thus the three axes were located on the CT scan or MR image of the patient's head via the same anatomical landmarks that were used to position the EEG electrodes.[22] The distance on the scalp between the nasion and inion on the midsagittal scout MRI slice was measured, and scalp positions 10% of the nasion-inion distance up from the nasion (FPZ) and the inion (OZ) and the midpoint of this distance (CZ) were marked. A line joining OZ and FPZ and a line perpendicular to this that cut through CZ were drawn. This intersection was the midpoint of the head and the origin of the coordinate system (0, 0, 0). We transferred this point to coronal and axial slices by determining the slice location closest to the origin on the midsagittal scout. The results obtained in all patients fitted very well to the midpoint of the head determined in a different study[23] in that the location was usually close to the bottom of the third ventricle, 5 mm anterior to the posterior commissure.

Because the head is not a perfect sphere as assumed by the inverse solution algorithm, we partially corrected for this shortcoming by applying proportional correction factors to the solution in the x, y, and z directions. The true head radii in each direction as determined from the patient's MRI were divided by the radius assumed by the inverse solution algorithm (10 cm), and this ratio was then multiplied by the x, y, and z solutions to yield values proportionally corrected for the patient's individual head shape. We then plotted these dipole locations in the MRI or CT relative to the origin that was previously located. This involved locating the closest slice in the desired axis, projecting the origin onto that slice, and moving the required distance away from the origin using the scale of the MRI. The orientation was expressed as the elevation and azimuth of the dipole, the latter the angular distance between the nasion the dipole.[4]

Estimation of Localization Error

We estimated the reproducibility, reliability, and validity of the inverse solution algorithm in the following ways. In the patients in whom multiple seizure onsets were evaluated, we determined the reproducibility by evaluating the variability between seizures of the dipole localization in the three axes. To test the reliability we started the inverse solution algorithm at different locations within the brain. The validity was evaluated by comparing the localization of the dipole to the localization of the lesion margin. The tissue in a spherical shell around the lesion is considered most likely to be the epileptogenic area, not the interior of the lesion itself,[12,13] except in the case of mesial temporal sclerosis. Because we had no means of knowing where in the shell was the true source of the epileptiform activity, we estimated the distance between the calculated dipole and both the closest and farthest lesion margins as the minimal and maximal errors for the dipole localization. In mesial temporal sclerosis we assumed that the epileptogenic zone stemmed from the hyperintense zone visible on proton density or T2-weighted images. Six patients were operated on, and their postoperative outcome was classified according to the Engel classification[24] and correlated to the dipole localization relative to the resection margin. In Patient 9, the preoperative MRI was not available; we assumed brain symmetry and plotted the dipole in the unoperated side and used these measurements in Table 1. Because the site of the maximum MR abnormality in the hippocampus was not known, we used the distance to the farthest end of the healthy hippocampus as the worst case value.

Results

We evaluated 20 seizure onsets containing a total of 414 sharp or slow waves in 4 patients (Patients 2, 8,

Table 1. Summary of Equivalent Dipole Localization Results in 12 Patients

Patient No.	Principal Diagnosis	EEG Event[a]	No. Events[b]	Distance to Lesion Margin (mm)[c]	
				Proximal[d]	Distal[d]
1	Astrocytoma	Spikes	24	5	22
2	Astrocytoma	Sz. onset	72	1	42
3	Dysplasia + gliosis	Spikes	144	8	18
4	Postoperative scar tissue	Spikes	20	8	49
5	Hemimegalocephaly	Spikes	22	1	62
6	Hemorrhage	Spikes	12	4	50
7	Poststroke atrophy	Spikes	14	5	56
8	Mes. temp. sclerosis	Sz. onset	88	0	5
9	Mes. temp. sclerosis	Spikes	23	6[e]	24[e]
10	Mes. temp. sclerosis	Sz. onset	133	0	2
11	Mes. temp. sclerosis	Spikes	18	4	12
12	Mes. temp. sclerosis	Sz. onset	38	0	4

[a]Activity evaluated (seizure onsets or interictal spikes).
[b]Number of spikes, sharp waves, or seizure (sz.) onset waveforms that were averaged.
[c]The distance is to the nearest and farthest lesion margins on the assumption that the epileptogenic zone is in the lesion capsule or in the hippocampus (mesial temporal [Mes. temp.] sclerosis patients). In Patients 2, 4, 5, 6, and 7 large lesions were present.
[d]The minimal and maximal error of our dipole modeling algorithm.
[e]No preoperative magnetic resonance image was available for Patient 9; we assumed brain symmetry and plotted the dipole in the unoperated side.

10, and 12) and a total of 277 interictal spikes in the other 8 patients. We were usually able to average more than 10 events during a single seizure onset. The average of the seizure onsets contained data from 38 to 133 events and so had a higher localization accuracy than a single event, in which only 7 to 44 sharp waves were evaluated. The inverse solution algorithm located the spike or seizure-onset dipole in reasonable proximity to the lesion in all cases. Table 1 shows the distances for each dipole location to the closest and farthest lesion margin as the best and worst case values for the dipole localization accuracy. However, the dipole solution was reliable in all cases; that is, starting at different points in the brain, especially starting at the most distal lesion margin and, in most cases, starting in the opposite hemisphere, did not change the dipole localization within the head. Localizations other than given here were always outside the head. Table 2 demonstrates the variation in localization between seven different seizure onsets in Patient 2, four different onsets in Patient 8, six different seizure onsets in Patient 10, and three different onsets in Patient 12. The maximal difference in localization between different inverse solutions as determined by the variability of localization of different seizure onsets was 2.5 cm. This variability occurred in the vertical (z) axis; in the other axes it did not exceed 1.8 cm. Table 3 is a summary of the source localization in all patients in respect to location and orientation of the equivalent dipoles. The *mean dipole elevation* in the 5 patients with mesial temporal sclerosis was 28 degrees; the dipole was directed medially in all patients. Table 4 shows all 6 patients who were operated on (Patients 2, 3, 8, 9, 10, and 12). The table demonstrates the relation between postsurgical outcome predictors[25] and the postoperative Engel classification.[24]

Table 2. Summary of Equivalent Dipole Localization Results from 20 Seizure Onsets in 4 Patients

Seizure	# Avg[a]	x[b]	y[b]	z[b]	Elevation[c]	Azimuth[c]
Patient 2						
1	7	2.3	−2.2	0.9	−82	45
2	14	2.7	−0.4	1.7	−70	146
3	9	3.9	−1.6	0.4	−79	270
4	17	[e]	[e]	[e]	[e]	[e]
5	12	3.2	−1.8	2.1	−73	180
6	22	2.8	−1.2	0.2	−81	45
7	8	2.4	−1.3	1.8	−79	270
Mean	12.0	2.9	−1.4	1.2	−77	159
Range	7–22	2.3–3.9	−0.4–−2.2	0.4–2.1	−82–−70	45–270
Patient 8						
1	44	1.3	−2.7	−0.8	42	243
2	18	[e]	[e]	[e]	[e]	[e]
3	14	1.6	−2.3	0.3	28	207
4	30	2.0	−2.8	−1.0	−4	219
Mean	29.3	1.6	−2.6	−0.5	22	223
Patient 10						
1	32	1.3	3.4	−0.5	−6	96
2	27	−0.1	3.7	0.8	5	121
3	22	[e]	[e]	[e]	[e]	[e]
4	25	0.8	4.0	0.8	0	96
5	21	0.5	3.1	−1.7	−20	113
6	28	0.1	3.8	0.2	−11	101
Mean	25.8	0.5	3.6	−0.1	−6	105
Range[d]	21–32	−0.1–1.3	3.1–4.0	−1.7–0.8	−20–5	96–121
Patient 12						
1	19	2.8	−5.4	−1.9	41	225
2	19	2.6	−5.5	0.7	30	259
3	26	[e]	[e]	[e]	[e]	[e]
Mean	22.5	2.7	−5.5	−0.6	36	242

[a]Number of sharp or slow waves averaged in the seizure onset.
[b]Equivalent dipole location in centimeters relative to the origin (0,0,0—approximately 5 mm anterior to the posterior commissure) (x = anteroposterior with + anterior; y = left-right with + left; z = vertical with + upward).
[c]The dipole orientation is expressed as Elevation (relative to the horizontal) and Azimuth (360 degrees clockwise from the nasion) after Ebersole and Wade (1991).
[d]The range of the results was maximal in the vertical axis (2.5 cm), presumably because no electrodes were present beneath the brain; in the other axes it did not exceed 1.8 cm. The localization error for these patients can be seen in Table 1.
[e]Either no result was obtainable from the given data or the result plotted outside the skull.

Table 3. Summary of Equivalent Dipole Localization in 12 Patients

Patient No.	Principal Diagnosis	EEG Event	Dipole Location[a]			Dipole Orientation	
			x	y	z	Elevation	Azimuth
1	Astrocytoma	Spikes	4.2	−1.3	2.2	70	56
2	Astrocytoma	Sz. onset	2.9	−1.4	1.2	−77	159
3	Dysplasia and gliosis	Spikes	−3.3	−4.0	−0.1	4	318
4	Postoperative scar tissue	Spikes	0.5	−7.4	1.3	0	281
5	Hemimegalocephaly	Spikes	6.7	−2.4	3.2	−16	197
6	Hemorrhage	Spikes	3.8	3.3	1.6	63	101
7	Poststroke atrophy	Spikes	−0.8	2.9	3.8	−49	215
8	Mes. temp. sclerosis	Sz. onset	1.6	−2.6	−0.5	22	223
9	Mes. temp. sclerosis	Spikes	1.9	−3.1	1.7	37	253
10	Mes. temp. sclerosis	Sz. onset	0.5	3.6	−0.1	−6	105
11	Mes. temp. sclerosis	Spikes	3.1	−2.3	−0.4	51	240
12	Mes. temp. sclerosis	Sz. onset	2.7	−5.5	−0.6	36	242

[a]In mesial temporal (Mes. temp.) sclerosis cases the dipole was always oriented medially and (with one exception) upward. No common pattern can be discerned in the other patients. See Tables 1 and 2 for an explanation of the column headings.

Table 4. Postsurgical Outcome in 6 Patients[a]

Patient No.	Principal Diagnosis	EEG Event	% EEG from Affected Side[b]	Follow-Up (mo)	Resection Size[c] (mm)	Engel Classification
2	Astrocytoma	Sz. onset	85[d]	23	[e]	IIA
3	Dysplasia + gliosis	Spikes	100	9	58[f]	IA
8	Mes. temp. sclerosis	Sz. onset	100	32	50	IA
9	Mes. temp. sclerosis	Spikes	100	28	45	IB
10	Mes. temp. sclerosis	Sz. onset	100	14	40	IA
12	Mes. temp. sclerosis	Sz. onset	100	6	40	IA

[a]This table demonstrates the relation between preoperative predictors of postsurgical outcome and the postoperative Engel classification (Engel et al, 1993) for all patients who underwent surgery. In all 6 the dipole localized into the resected area. Four of 6 patients remained seizure free; Patient 9 experienced auras on dose reduction, and Patient 2 had two spells over 2 years.
[b]How many seizures or spikes arose from the resected tissue.
[c]Measured from the anterior temporal tip.
[d]Six of seven seizures arose in the right frontal lobe; the seventh appeared to arise on the left but was obscured by muscle artifact.
[e]A frontal and temporal lobectomy was performed.
[f]The resection margin started 80 mm posterior to the anterior temporal tip and 58 mm was resected.

Patient 3

This 23-year-old man had frequent (6–10/mo) tonic-clonic seizures since the age of 8 years characterized by dystonic posturing of the left arm with secondary generalization. MRI showed a nonenhancing, T1-dark, T2-bright abnormal signal focus in the right occipito-temporal junction region suggestive of cortical gliosis. The EEG contained frequent spikes with a phase reversal at T6 (Fig 1). One hundred forty-four of these spikes were evaluated. The dipole localized 0.8 cm superior to this lesion in the gray matter/white matter junction of the posterior temporal lobe (Fig 2). The patient underwent intracranial monitoring with subdural grid electrodes. Seizures demonstrated a clear pattern of origin from the electrode leads located in the vicinity of the MRI abnormality, 0.8 cm away from the estimated dipole localization. At surgery, the inferior and middle temporal gyrus 8 cm back from the anterior temporal tip were removed. The dipole localized in the resected area. Surgical pathology revealed dysplastic gray matter with focal gliosis. The patient is seizure-free at 1 year after surgery (Engel Ia).

Patient 10

This 42-year-old woman had a long history of complex partial seizures, occasionally with left hand movements. MRI showed minimal hyperintensity seen on coronal proton-density images in the left hippocampal formation. A positron emission tomographic scan showed hypometabolism in the left temporal lobe. Six seizures were recorded during video/EEG telemetry with onset from the left frontotemporal region with initial 3- to 4-Hz 200-μV rhythmic slow activity with higher amplitude on T3 and F7 leads for up to 12 seconds (Fig 3). From the six seizure onsets, five could be evaluated (see Table 2) (1 seizure did not start with rhythmic activity). The variability in the three directions was 0.5 cm (anteroposterior), 0.3 cm (left-right), and 0.9 cm

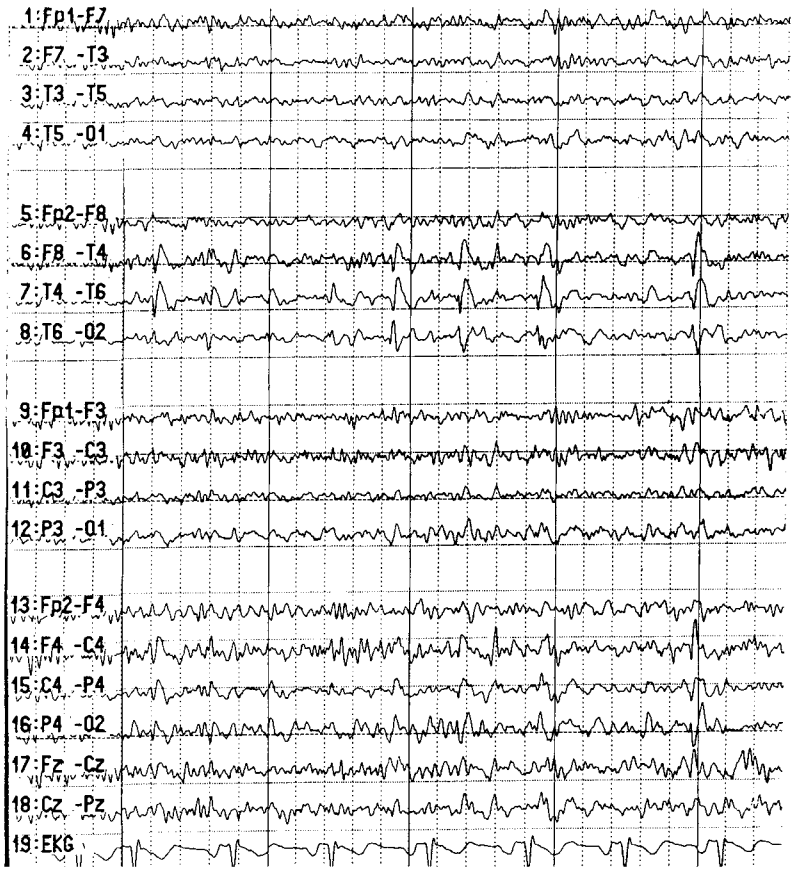

Fig 1. EEG of Patient 3 showing multiple spikes in the right posterior temporal region with phase reversal at T6, 144 of which were marked, aligned, superimposed, and averaged for localization. One small division is 200 msec; the last spike in the F8-T4 channel has a peak-to-peak amplitude of 50 μV.

(superoinferior). The averaged dipole localized into the left anterior hippocampus (Fig 4). During brain surface ECoG no spiking was recorded. However, when a depth electrode was inserted into the patient's hippocampus according to the dipole localization that was plotted on the MRI in the operating room, frequent spike discharges were recorded only from the deepest contact of the depth electrode. The depth electrode was tracked after excision of the temporal neocortex and was seen to extend directly in the anterior portion of the hippocampus. The resected tissue included the dipole localization, and pathological study of the left hippocampus showed focal subpial (Chaslin's) gliosis. The patient was seizure-free at 3 years (Engel Ia).

Discussion

Although dipole source localization has been widely used in various research and clinical settings, our report here is the first consecutive series of patients with diverse intracerebral lesions evaluated with EEG dipole source analysis.

Factors Concerning Reliability, Reproducibility, and Validity

We previously tested the accuracy of our inverse solution algorithm and plotting techniques by creating artificial dipoles in patients undergoing invasive intracranial monitoring with depth electrodes.[9] These data demonstrated a good correlation between the calculated source and the artificially created dipole. We found a mean localization error of 13 mm, with a maximum localization error of 18 mm. Hence, we were able to validate the ISA invasively and our results were in general agreement with similar experiments performed previously.[6–8] With the patient data presented here we begin to validate the inverse solution algorithm clinically.

Localization accuracy was assessed in four ways: (1) by determining the variability of dipole localization of different seizure onsets within a subject, irrespective of the lesion localization (reproducibility of the results); (2) by starting the ISA at different points in the head—that is, on the contralateral hemisphere (reliability of the results); (3) by estimating the dipole localization relative to the lesions with which the spikes and

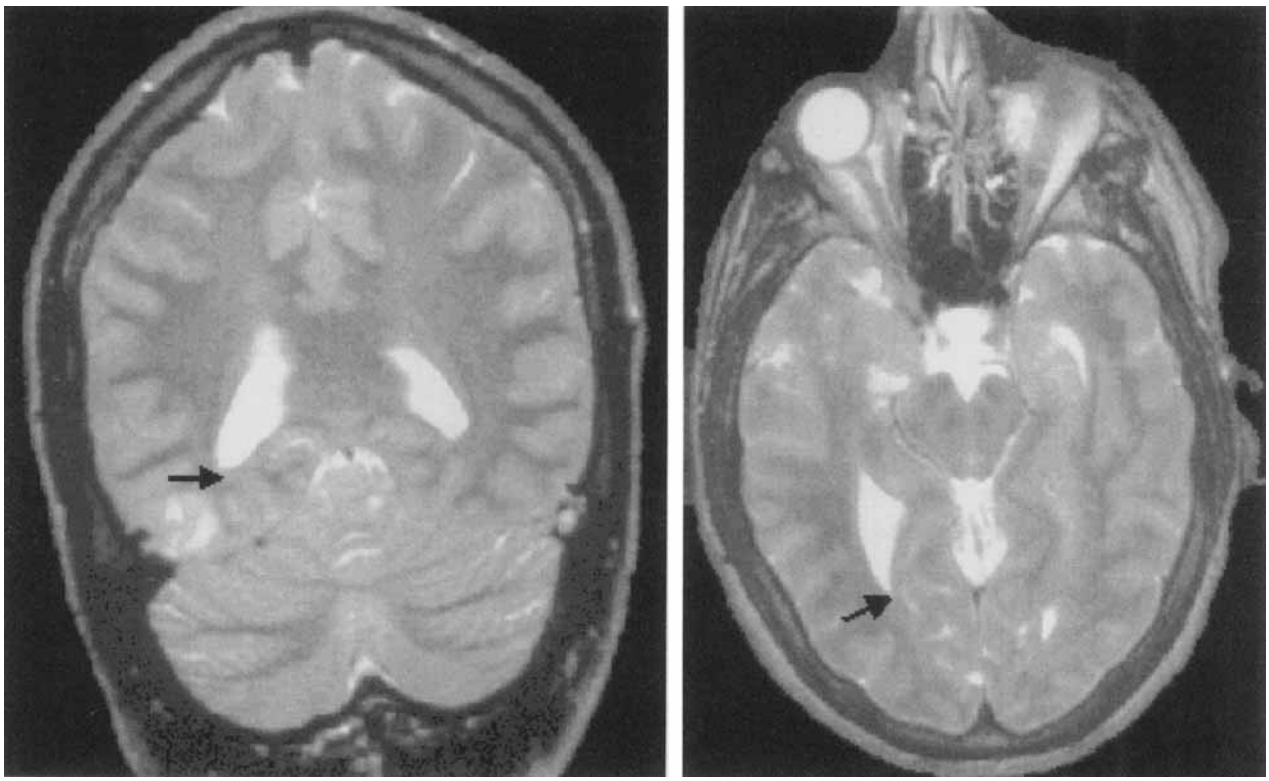

Fig 2. T2-weighted coronal and axial MRI showing the dipole localization for Patient 3. The dipole origin is at the tail of the arrow with the head denoting direction. The dipole localized 0.8 cm superior to the T2 hyperintensity, which is seen on the coronal image at the gray-white matter junction of the temporooccipital region.

sharp waves were associated (validity of the results); and (4) by relating localization relative to the clinical outcome in patients undergoing surgery.

REPRODUCIBILITY. The variability between solutions for different seizure onsets in the same patient did not exceed 2.5 cm. The highest intrasubject variability was observed in the vertical direction, presumably because no recording electrodes were present beneath the brain to constrain the localization in this axis. In the anteroposterior and the left-right directions the maximum variability did not exceed 1.8 cm. Presumably, this variability is due to background noise in the EEG and could be compensated for by increasing the number of averaged events.[9]

RELIABILITY. Starting the ISA at different points in the head (eg, in the contralateral hemisphere) did not change the localization of the modeled dipole, which was an indicator of their robustness. However, the reliability of the results can also be further increased by increasing the number of averaged events.[9] When evaluating rhythmic activity or repetitive sharp waves during a seizure onset the number of averaged events is limited by the onset of muscle artifacts on the EEG as the seizure progresses. We were usually able to average EEG events from multiple seizure onsets. The average of the seizure onsets contained more data and so had a higher localization accuracy than did a single seizure onset.

VALIDITY. Testing the validity of our results, we found a reasonable distance between the lesion margin and the estimated dipole source in all patients. Lateralization of the computed electrical source of both the spikes and the seizure onset was to the hemisphere affected by the lesion. In patients with proven mesial temporal sclerosis the dipole localized into the hippocampal area of the affected hemisphere. In patients with intracerebral lesions other then mesial temporal sclerosis, we assumed that the source of the epileptiform activity was in the shell of tissue surrounding the lesion.[12,13] However, it was impossible to know which portion of the shell was the electrical source generator of the epileptiform activity and an exact determination on the localization accuracy was only obtained from two patients. In Patient 10, the accuracy of the ISA was proven directly by placement of a depth electrode intraoperatively into the region where the algorithm computed the dipole, which demonstrated that the

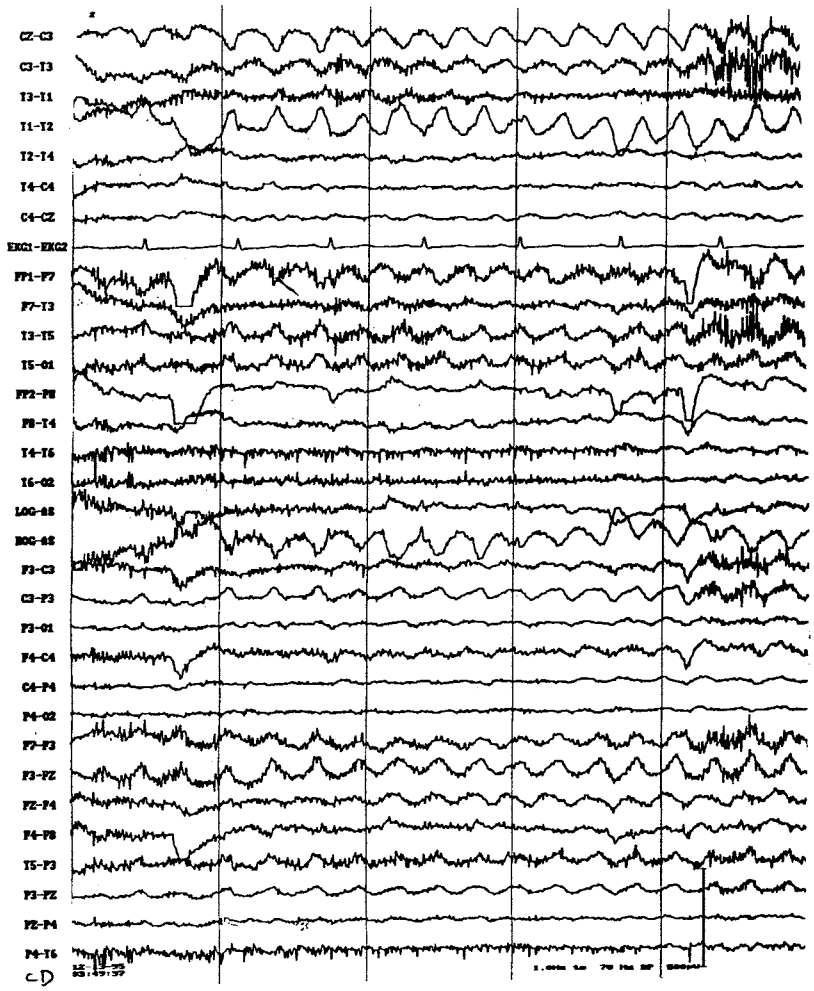

Fig 3. EEG of Patient 10 showing 3- to 4-Hz sharp and slow wave activity at seizure onset in the left frontotemporal region. The patient had no interictal activity, and no spiking was seen during ECoG. When a depth electrode was inserted into the left hippocampus, indicated by dipole localization, frequent spiking was present that did not propagate to the cortex. The calibration mark is 500 μV; one division is 1 second.

spikes were generated from within this area. In Patient 3, a subdural grid was placed over the lesion and the source of the spikes determined by chronic recordings to be within 8 mm of the dipole localization. These values correspond well to the accuracy determined by using the ISA on artificial dipoles.[7-9]

To evaluate the localization accuracy in patients without invasive recordings, we measured the distances from the computed dipole to the closest and farthest lesion margin as revealed by CT or MRI, which represent the best and worst case solutions of the dipole localization. The large lesions of Patients 1, 4, 5, 6, and 7 spoil the otherwise good results of even the "worst case" solution. In those patients who had scar tissue, tumors, or cavitary changes, the inverse solution algorithm never localized the spike into the lesion but always to its margin. If there was a random variability of more than 1 cm, some of the solutions would have located to within the lesion. Because this was not seen, the validity of the solutions is thereby reinforced.

Localization Errors

The localization error in this study is presumably due to a combination of placement errors of the EEG electrodes, signal noise, and artifacts; the use of an inexact model of the head (4 sphere model); and inaccuracies when plotting the dipoles on the respective MR images. We think that electrode location errors average out over the 21 electrodes because they are random, and we do not consider that further localization accuracy here (ie, with digitizers) will produce a significant overall improvement. Cohen and colleagues[7] assumed that the main source of localization error (ie, 6 mm) was due to the inexact model of the head. When comparing a three-sphere model with a realistically shaped head model, Roth and co-workers[10] found that localization obtained with the latter corresponded better to localization obtained during ECoG. Presumably, the localization accuracy would improve if we would use a realistically shaped head model. We partly corrected for this shortcoming by applying proportional correction

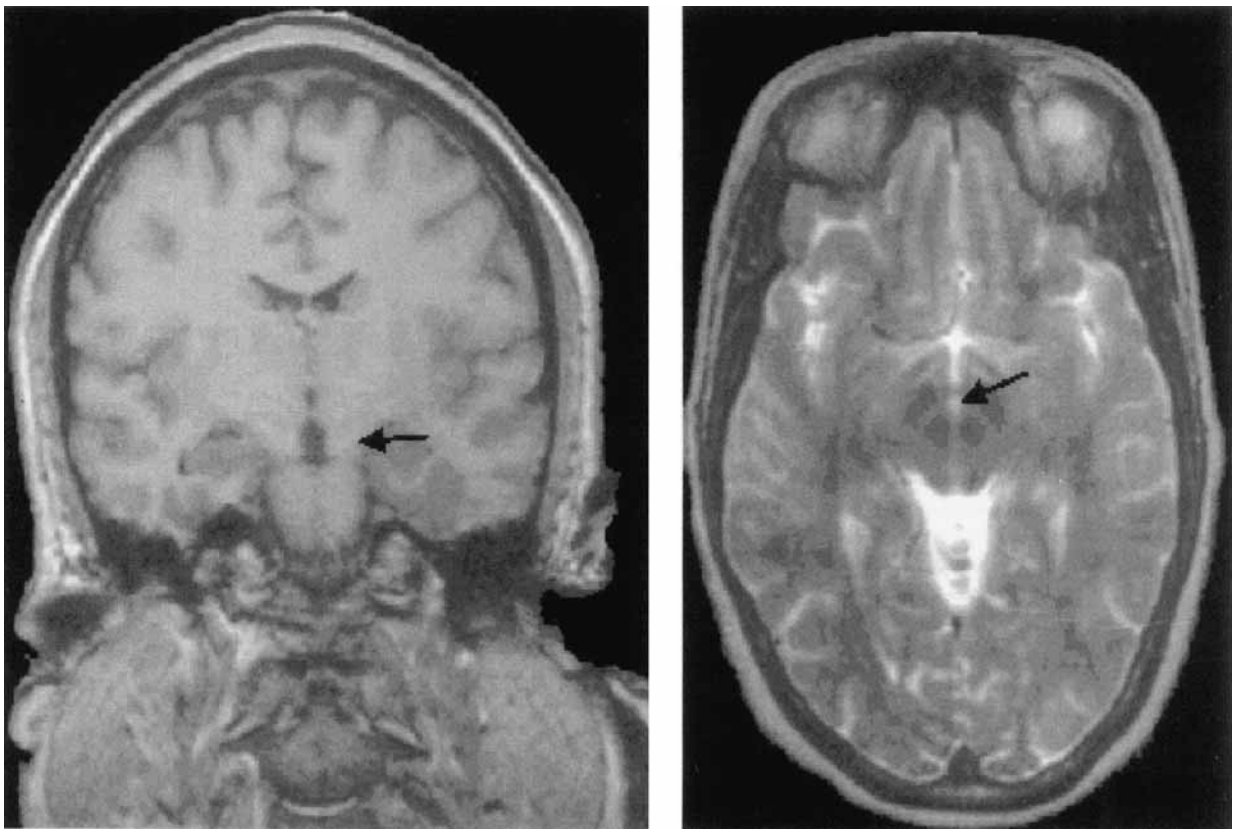

Fig 4. Dipole localization for Patient 10 averaged from six seizure onsets. Localization to the left hippocampal region was suggested during surgery by a depth electrode inserted into the presumed epileptogenic area that showed frequent spiking. After anterior temporal lobectomy the patient remained seizure-free.

factors to the solutions that we have previously shown to improve localization errors by up to 20%.[9]

Problems of the Inverse Solution Algorithm

There is debate concerning whether scalp electrodes can register electric fields generated in deep structures at sufficient amplitudes for source modeling[26–28] and whether the potentials recorded at the scalp are largely generated in superficial neocortex by epileptiform activity propagated from distant, deep foci.[28–31] Figures 2 and 4 of Alarcon and associates[28] clearly show examples of deep activity that are associated with simultaneous events in surface recordings. In spite of these data, Alarcon and associates[28] have concluded that physiologically unrealistic voltage gradients (>1,000 μV in 2.5 mm), and hence source strengths, are required for deep sources to produce scalp potentials that can be readily detected. However, such large voltage gradients need only occur for deep sources if the sources are assumed to be focal (ie, dipolar). It can be shown with solid angle calculations[27] that a distributed source with the shape of a disc and a diameter of 3 cm can produce scalp potentials that are in the range of epileptic spikes but that have gradients of less than 1,000 μV in 2.5 mm. The reason for this is that the potential of a disc source decreases much more slowly with distance than for a dipolar disc. For example, if a dipolar and a 3-cm disc source both have the same potential at a distance of 0.1 cm from the sources, the potential produced by the dipole at a distance of 5 cm will be only 0.04% of that at 0.1 cm but the disc potential will be 4.54%. Regarding propagation, our patients with mesial temporal sclerosis had their dipoles localized to the hippocampus by the ISA. It could be said that hippocampal epileptiform activity propagated to the temporal neocortex and activated it in such a distribution that the equivalent dipole localized to the hippocampus. But this explanation would not readily account for the reasonable localization of the dipoles associated with the variety of lesions and their sites in the remainder of our patients because it seems unlikely that the required neocortical activation would occur in all cases.

In 4 of 20 seizure-onset evaluations the ISA was unable to calculate a reasonable localization of a dipole to fit the given data. Possible explanations include the superimposition of muscle artifacts and rapid spreading of the seizure activity. Emerson and co-workers[29]

found that seizure activity can propagate at very high velocities from the anterior to the posterior temporal lobe or the frontal lobe using inherent neuronal circuits. In these cases the ISA is presumably not able to calculate a single moving dipole from the given data. Barth and colleagues[32] demonstrated that the sequential activation of spatially distributed sources can constitute a single EEG event (ie, spikes or sharp waves). However, the ISA uses these data to calculate one equivalent dipole source in the brain. Thus, if multiple source generators are present in the brain, the program will calculate a single "equivalent" localization that might have no relationship to the real sources and even might localize to nonsense areas.[28] To minimize this problem we excluded patients who demonstrated multiple spike foci or diffuse pathology. A related problem is that the inverse solution algorithm calculates point sources, not epileptogenic areas. Pathological neuronal populations that might be distributed over a large spatial area in the brain are falsely demonstrated as a single source. Moreover, activity that spreads over the complicated folded gyral anatomy might distort the surface EEG. For example, electrical activity over different banks of a sulcus might cancel out and result in a zero potential on the surface,[33] which might give an erroneous impression regarding the source of epileptic activity in the brain. Finally, the EEG might show epileptogenic activity, and the ISA produces a good solution when this activity is in an area secondarily triggered by abnormal impulses propagated from a relatively distant source. This would constitute an erroneous localization with respect to the origin of the clinical seizure. Despite these limitations and the inherent oversimplification of the ISA solution, it appears that the spike topography contains substantial information about which parts of the temporal lobes are involved in the epileptogenic process.[31]

Assessment of dipole orientation has been used to differentiate between neocortical and mesial temporal seizure onset,[4] the latter having a mean dipole elevation of 42 degrees (±5) and the former 2 degrees (±10). Our patients with mesial temporal seizures had a mean dipole elevation intermediate between these values, possibly related to our smaller sample size. The dipole azimuths in our patients were roughly similar to those of Ebersole and Wade.[4] Comparisons of EEG and ECoG have shown that EEG source analyses are able to localize epileptogenic areas in the clinical settings.[10,11] Our findings are in concordance with those studies.

Future Implications

Dipole localization might help differentiating benign and epileptogenic spikes. Preliminary results from our laboratory suggest that benign epileptiform transients of sleep have a completely different pattern of localization from the spikes present in mesial temporal sclerosis.

Our data are consistent with those of Ebersole and Wade,[4] who found that patients with mesial temporal sclerosis had spikes with oblique dipoles and patients with cortical lesions, both discrete and multifocal, had spikes with radial dipoles. Because the EEG registers radial dipole components whereas magnetoencephalography does not, the EEG is at least complementary with magnetoencephalography.[34] The relative usefulness of these two techniques in the clinical evaluation of epileptic patients has not yet been clearly delineated.

Accurate localization of seizure onset is the basis for successful surgery and is derived from the convergence of diverse investigations.[35] Two possible clinical applications of EEG dipole source localization may be to provide additional localizing information and to guide the placement of invasive intracranial electrodes when these are necessary. In the 6 patients who underwent surgery, the dipole localized to the resected area and 4 of 6 patients remained seizure-free after surgery (Engel Ia). However, postoperative follow-up was too short for most patients to make any assumptions on long-term outcome.[36] Cascino and associates[37,38] found that, although routine EEG findings correlated with the temporal lobe of seizure origin, there was no significant relation to the operative outcome. Alarcon and coworkers[39] have shown a good correlation of outcome with excision of regions where discharges on ECoG show the earliest peaks ("leading regions"). However, our refined method of scalp EEG source localization might add information that improves postsurgical outcome and warrants further study.

Dr Krings was supported by the Biomedical Sciences Exchange Program and the Konrad Adenauer Foundation.

We are grateful to Andrew M. Roy for his excellent work in designing the spike averaging software, Rosamund A. Hill for software assistance, and Kara J. Houghton for technical assistance.

References

1. Scherg M, von Cramon D. Two bilateral sources of the late AEP as identified by a spatio-temporal dipole model. Electroenceph Clin Neurophysiol 1985;62:32–44
2. Buchner H, Scherg M. Analyse der Generatoren früher kortikaler somatosensibler evozierter Potentiale (N. medianus) mit der Dipolquellenanalyse: Erste Ergebnisse. Z.EEG-EMG 1991; 22:62–69
3. Scherg M. Functional imaging and localization of electromagnetic brain activity. Brain topography 1992;5:103–111
4. Ebersole JS. EEG Dipole modeling in complex partial epilepsy. Brain Topography 1991;4(2):113–123
5. Ebersole JS, Wade PB. Spike voltage topography identifies two types of fronto-temporal epileptic foci. Neurology 1991;41: 1425–1433
6. Smith DB, Sidman RD, Flanigin H, et al. A reliable method for localizing deep intracranial sources of the EEG. Neurology 1985;35:1702–1707

7. Cohen D, Cuffin BN, Yunokuchi K, et al. MEG versus EEG Localization Test using implanted sources in the human brain. Ann Neurol 1990;28:811–817
8. Cuffin BN, Cohen D, Yunokuchi K, et al. Test of EEG localization accuracy using implanted sources in the human brain. Ann Neurol 1991;29:132–138
9. Krings T, Cochius JI, Connolly S, et al. Accuracy of EEG Dipole localization using implanted sources in the human brain. Neuroimage 1996;3:S138
10. Roth BJ, Ko D, von Albertini-Carletti IR, et al. Dipole localization in patients with epilepsy using the realistically shaped head model. Electroenceph Clin Neurophysiol 1997;102:159–166
11. Nakasato N, Levesque MF, Barth DS, et al. Comparisons of MEG, EEG, and ECoG source localization in neocortical partial epilepsy in humans. Electroenceph Clin Neurophysiol 1994;171:171–178
12. Boon PA, Williamson PD, Fried I, et al. Intracranial, intraaxial, space-occupying lesions in patients with intractable partial seizures: an anatomoclinical neuropsychological and surgical correlation. Epilepsia 1991;32:467–476
13. Cascino GD, Boon PA, Fish DR. Surgically remediable lesional syndromes. In: Engel J Jr, ed. Surgical treatment of the epilepsies, 2nd ed. New York: Raven Press, 1993:77–87
14. Ropper AH, Chiappa KH, Grass ER. A practical non-cephalic reference electrode: the Stephenson-Gibbs non-cephalic system. Clin Electroenceph 1978;9:140–143
15. Cuffin BN. A comparison of moving dipole inverse solutions using EEGs and MEGs. IEEE Trans Biomed Engr 1985;32: 905–910
16. Sidman RD, Baker Kearfott R, Major DJ, et al. Development and application of mathematical techniques for the non-invasive localization of the sources of scalp-recorded electric potentials. In: Eisenfeld J, Levine DS Witten M, eds. Biomedical Modeling and Simulation. Amsterdam: Elsevier, 1989:133–157
17. Schneider MR. A multistage process for computing virtual dipolar sources of EEG discharges from surface information. IEEE Trans Biomed Engr 1972;19:1–19
18. Cuffin BN. Effects of measurement errors and noise on MEG moving dipole inverse solutions. IEEE Trans Biomed Engr 1986;33:854–861
19. Okada Y. Discrimination of localized and distributed current dipole sources and localized single and multiple sources. In: Weinberg H, Stroink G, Katila T, eds. Biomagnetism: applications and theory. New York: Pergamon Press, 1985:266–272
20. Cuffin BN, Cohen D. Comparison of the magnetoencephalogram and electroencephalogram. Electroenceph Clin Neurophysiol 1979;47:132–146
21. Murro AM, Smith JR, King DW, Park YD. Precision of dipole localization in a spherical volume conductor: a comparison of referential EEG, magnetoencephalography and scalp current density methods. Brain Topography 1995;8:119–125
22. Lagerlund TD, Sharbrough FW, Jack CR, et al. Determination of 10-20 system electrode locations using magnetic resonance image scanning with markers. Electroenceph Clin Neurophysiol 1993;86:7–14
23. Towle VL, Bolanos J, Suarez D, et al. The spatial location of EEG electrodes: locating the best-fitting sphere relative to cortical anatomy. Electroenceph Clin Neurophysiol 1993;86:1–6
24. Engel J Jr, van Ness PC, Rasmussen TB, Ojemann LM. Outcome with respect to epileptic seizures. In: Engel J Jr, ed. Surgical treatment of the epilepsies. 2nd ed. New York: Raven Press, 1993:609–621
25. Armon C, Radtke RA, Friedman AH, Dawson DV. Predictors of outcome of epilepsy surgery: multivariate analysis with validation. Epilepsia 1996;37(9):814–821
26. Cooper R, Winter AL, Crow HJ, Walter WG. Comparison of subcortical, cortical and scalp activity using chronically indwelling electrodes in man. Electroenceph Clin Neurophysiol 1965; 18:217–228
27. Gloor P. Neuronal generators and the problem of localization in electroencephalography: application of volume conductor theory to electroencephalography. J Clin Neurophysiol 1985;2: 327–354
28. Alarcon G, Guy CN, Binnie CD, et al. Intracerebral propagation of interictal activity in partial epilepsy: implications for source localization. J Neurol Neurosurg Psychiatry 1994;57: 435–449
29. Emerson RG, Turner CA, Pedley TA, et al. Propagation patterns of temporal spikes. Electroenceph Clin Neurophysiol 1995;94:338–348
30. Emerson RG, Turner CA. The relationship between spikes recorded simultaneously from hippocampus, cortex and scalp. Presented at annual meeting of American Clinical Neurophysiology Society, Beverly Hills, CA, September, 1997. J Clin Neurophysiol (in press)
31. Lantz G, Holub M, Ryding E, Rosen I. Simultaneous intracranial and extracranial recording of interictal epileptiform activity in patients with drug resistant partial epilepsy: patterns of conduction and results from dipole reconstructions. Electroenceph Clin Neurophysiol 1996;99:69–78
32. Barth DS, Sutherling WW, Engel Jr J, Beatty J. Neuromagnetic evidence of spatially distributed sources underlying epileptiform spikes in the human brain. Science 1984;223:293–296
33. Jayakar P, Duchowny M, Resnick TJ, Alvarez LA. Localization of seizure foci: pitfalls and caveats. J Clin Neurophysiol 1991; 8:414–431
34. Wieringa HJ, Peters MJ, Lopes da Silva FH. The estimation of a realistic localization of dipole layers within the brain based on functional (EEG, MEG) and structural (MRI) data: a preliminary note. Brain Topography 1993;5:327–330
35. Engel J Jr, Henry T, Risinger MW, et al. Presurgical evaluation for partial epilepsy: relative contributions of chronic depth electrode recordings versus FDG-PET and scalp-sphenoidal ictal EEG. Neurology 1990;40:1670–1677
36. Spencer SS. Long-term outcome after epilepsy surgery. Epilepsia 1996;37:807–813
37. Cascino GD, Trenerry MR, So EL, et al. Routine EEG and temporal lobe epilepsy: relation to long-term EEG monitoring, quantitative MRI, and operative outcome. Epilepsia 1996;37: 651–656
38. Cascino GD, Trenerry MR, Jack CR et al. Electrocorticography and temporal lobe epilepsy: relationship to quantitative MRI and operative outcome. Epilepsia 1995;36:692–696
39. Alarcon G, Garcia Seoane JJ, Binnie CD, Martin Miguel MC, Juler J, Polkey CE, Elwes RDC, Ortiz Blasco JM: Origin and propagation of interictal discharges in the acute electroencephalogram. Implications for pathophysiology and surgical treatment of temporal lobe epilepsy. Brain 1997;120:2259–2282